Available online at www.sciencedirect.com

ScienceDirect

Procedia Manufacturing 00 (2019) 000–000

Procedia MANUFACTURING

www.elsevier.com/locate/procedia

5th International Conference on System-Integrated Intelligence

Towards self-healing biomimetic hair flow sensor

Minerva G. Vargas Gleason[a]*, Walter Lang[a]

[a]*IMSAS, University of Bremen, Otto-Hahn-Allee 1, Bremen 28213, Germany*

* Corresponding author. Tel.: +49 421 218 62638. *E-mail address:* mvargas@imsas.uni-bremen.de

Abstract

Some of the most sensitive sensors seen in nature are flow sensors. These consist of small hairs with receptors at the base that detect when the hair deflects. Artificial hair flow sensors try to mimic this response, creating small sensitive systems. However, the drawback of these sensors is, that if the hair break, the sensor is unusable. This paper presents the sensing part of a biomimetic artificial hair sensor, that can grow and regrow the hair if it gets damaged. The system consists of a sensor system with an extrusion channel for a hair, where a polymeric hair can be extruded. The sensing elements are four strain gauges embedded in a flexible substrate that lean on the base of the artificial hair while still allowing it to grow. The presented system is able to detect the direction of the hair bending and, therefore, detect the direction of the flow that surround the sensor.

Keywords: Artificial hair; biomimetic; flow sensor; microsystems; sensors; sensor array

1. Introduction

In nature, we can find extraordinary sensor systems that are used as inspiration to create new, highly sensitive systems using biomimetics. Hair flow sensors in animals have a simple working principle, high performance and sensitivity. These consist of small hairs that bend when a flow is present and, due to the viscous drag, activate receptors on the base of the hair.

Arrays of hairs are used in nature not only to directly detect flow, but also for acoustic sensing, navigating through complex surroundings and for tactile sensing.

Arthropods, such as spiders and crickets, use arrays of 500 to 750 filiform hairs to sense air currents and detect preys or predators [1] [2]. Fish use small hair receptors in their lateral line system (LLS) to detect water currents and avoid collisions while swimming [3]. Bats use small hairs in their wings to monitor the air currents and improve flight control [4].

1.1. State of the art

Artificial hair sensors attempt to mimic the fast response and high sensitivity of these natural sensors.

McConney et al. developed a bioinspired hydrogel capped hair sensory system that mimics the LLS of fish [3]. The fabricated hair was 825 µm long, with a synthetic cupula over the last 550 µm to improve the viscous drag. This system can detect both acceleration and velocity of a surrounding flow even when the water is almost stationary.

Ya-Feng Lui et al. created an electronic skin with an array of nylon hairs capable of detecting multiple signals of pressure, surface roughness, and the direction and intensity of air currents just as the human skin [5].

An array of hair sensors has been used for acoustic flow measurements, where the directivity of the sound can be measured. This system consists of an array of 1mm long SU-8

hairs coupled with a capacitive sensor. The sensors are used for acoustics [6].

A similar array of capacitive artificial hair sensors was used by Dagamesh et al. for high resolution air flow pattern observation with a detection limit of 1 mm/s, providing a 52% improvement compared to previous systems [7].

One drawback of all the mentioned artificial hair sensors is that if the hair breaks due to an external force, the sensor cannot operate any more and has to be replaced. Due to this reason, this type of sensors is not commercially available.

2. Concept

This paper presents the novel idea of fabricating a flow sensor that mimics the filiform hairs in animals, having a system that can grow and regrow a hair if it gets damaged. In this way, the sensor must not be replaced if the hair breaks. The sensors will be able to detect when this happens and extrude a new hair.

The proposed system is shown in Fig. 1a, it is divided in two parts. The first part is comprised by the sensing elements located on the base of the hair, which can detect when the hair bends, the magnitude and direction of the bending and can determine if the hair broke. Using this information, the flow that caused the hair to bend can be calculated. The second part of the system is in charge of the hair growth and consists of a reservoir full of polymer, an extrusion system and an extrusion channel.

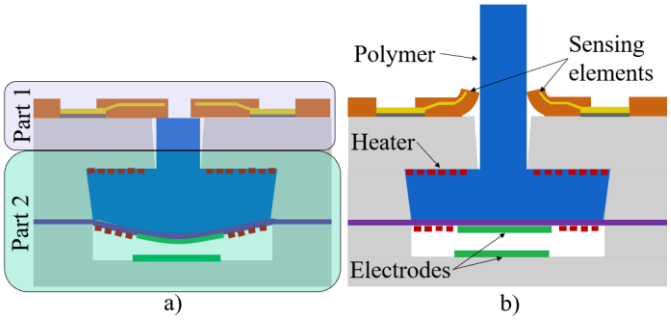

Fig. 1. The system is divided in two: Part 1: Sensing. Part 2: Hair growing. a) Before hair growth. b) After hair growth.

Fig. 1b shows one possible system for growing the hair (part 2) using heaters to melt the polymer stored in the reservoir and pushing it out of the extrusion channel by bending a silicon nitride membrane with two electrodes. Several approaches are being researched and the best method will be presented in a future publication.

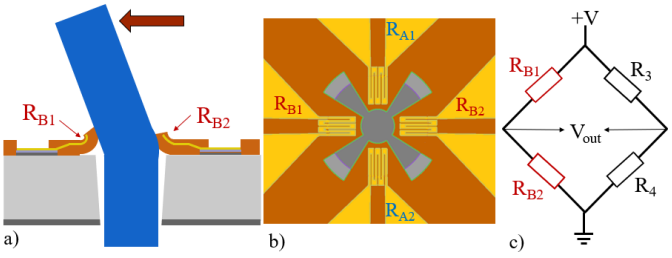

Fig. 2 Sensing a) Side view of hair being deformed, here R_{B1} increases, R_{B2} decreases, R_{A1} R_{A2} remain constant. b) Top view of the strain gauges. The extrusion channel is dark gray. c) Two strain gauges arranged in a Wheatstone bridge with two fixed resistors.

In this paper, we will focus on the sensing part of the system (part 1). This consists of four strain gauges embedded in a flexible substrate that lean on the base of the hair.

The system is designed in such a way, that the polymer hair can grow and regrow from the extrusion channel and the sensing elements remain in contact with the new hair, as seen in Fig. 2a. Therefore, the sensing elements (strain gauges) must be embedded in a flexible substrate above the extrusion channel as seen in Fig. 2b.

The strain gauges are arranged as pairs in the X and Y axis (perpendicular to the hair), as shown in Fig. 2b. When the hair is bent to one side, assume in X-direction, the two strain gauges located in this axis will suffer a change in resistance.

Each resistor pair is arranged in a Wheatstone bridge, using two external fixed resistors to complete the bridge (see Fig. 2c). This configuration consists of two “branches” (two resistors in series) connected in parallel between voltage and ground. When the value of one resistance changes, an output voltage can be measured [8]. The advantages that the Wheatstone bridge gives are that even small changes in resistance can be detected and that temperature compensation is automatically obtained [9].

The voltage output of this bridge is then connected to an amplification circuit that uses an instrumentation amplifier to filter out noise and amplify the voltage by a factor of 10.

3. Fabrication

The sensors were fabricated in a cleanroom using standard silicon microtechnology. As substrate, a double side polished 375 µm thick silicon wafer was used. A 500 nm thick silicon oxide layer was thermally grown for electrical insulation. Titanium and gold were sputtered (see Fig. 3a) and structured to create the contact pads, the SiO_2 was also etched (see Fig. 3b). For the flexible substrate, a 5 µm thick polyimide (PI) layer was spin coated and openings for the contact pads were etched, the borders were smoothed using high temperature (see Fig. 3c).

A 100 nm thick metallization layer was sputtered and structured to create the strain gauges. In this step, two versions were made, one with gold and one with platin as material for the sensors. On top, a thin 2 µm PI layer was spin coated as insulation and protection for the strain gauges (see Fig. 3d).

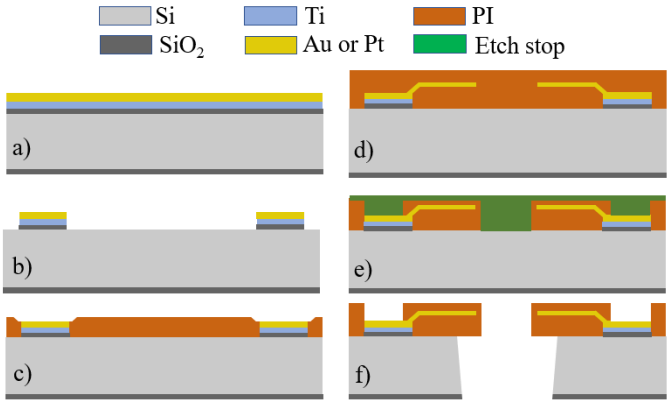

Fig. 3 Sensor fabrication.

The PI layers were structured to open the contact pads and to leave place for the hair to grow. A sacrificial layer of photoresist was spin coated as etch stop for the back side etching of the extrusion channel, as shown in Fig. 3e. Finally, the SiO_2 and the silicon were etched from the bottom side of the wafer to create the extrusion channel for the hair (see Fig. 3f).

Notice that the PI layer with the embedded strain gauges remain as free-floating structures on top of the extrusion channel, as seen in Fig. 2b. These structures will bend upwards and lean on the hair.

The average thickness of a human hair is 75 µm, but it can be as thick as 181 µm [10]. The diameter of the extrusion channel was also varied in this range, sensors with an extrusion channel of 80 µm, 100 µm, and 120 µm in diameter were designed.

Several strain gauges geometries were fabricated in both Au and Pt to determine which design has a good compromise between sensitivity and stability. Table 1 shows the different geometries that were fabricated.

For the orientation of the strain gauges, two configurations were made of each sensor type: one with gauges parallel to each other (see Fig. 2b and Fig. 5) and other with gauges radial to the extrusion channel (see Fig. 12). However, this seems to have no influence in the measurement results.

Table 1. Different sensor geometries. The diameter of the extrusion channel and the length of the strain gauges were varied. For all variations, sensors with Au and Pt as material for the strain gauges were manufactured.

Diameter (µm)	Length (µm)
80	10
	15
	20
	30
100	10
	15
	20
	30
120	10
	15
	20
	30

The finished sensors are diced in 2 mm × 2 mm chips.

4. Measurements and results

In order to test the sensor and determine its characteristics, a hair replacement was used. The requirements for the hair were a thin, flexible filament.

Our first approach was using an insulated 100 µm thick copper wire from BLOCK[1]. It was thin enough to pass though the extrusion channel of the 120 µm sensors. However, while manipulating the sensor, it easily bent 90° at the base, breaking the strain gauges.

A suture monofilament from AgnTho's AB[2] proved to be a better option. The ETHILON* (Polyamide 6) suture in gauges size 7-0 and 6-0 was used as hair filaments for the sensors with 100 µm and 120 µm extrusion channel, respectively.

Since the above-mentioned filaments did not fit in the sensors with an 80 µm extrusion channel and manipulating a thinner filament was complicated, it was decided to exclude these sensors and focus on the 100 µm and 120 µm ones.

For the measurements, the sensor was arranged in two Wheatstone bridges, one to measure the flow in the Y direction (Channel A) and one in the X direction (Channel B).

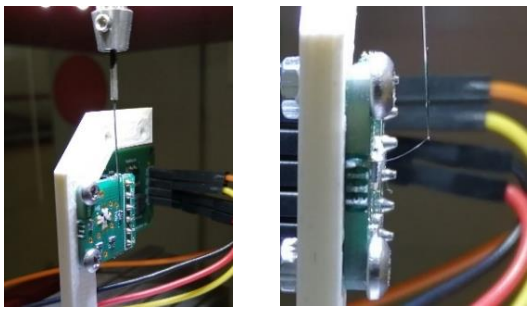

Fig. 4 Measurement setup. Channel B, stage two is being tested.

The measurements were carried out in a Condor 100 bond tester from XYZTEC[3]. The sensor was fixed to a 3D printed holder where the orientation of the sensor can be changed. A thin metallic hook was used to pull the hair 3 mm upwards (see Fig. 4). This test allows us to repeatably deform the hair in a given direction and maintain this deformation to analyze the stability of the strain gauges under strain. The hair was deformed between four and five times per measurement.

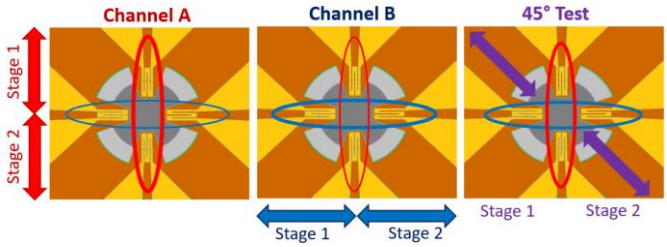

Fig. 5 Directions of the hair deflection during measurement: Channel A stage 1 and 2 (90° and 270°), Channel B stage 1 and 2 (180° and 0°) and a test at 45°, stage 1 and 2 (135° and −45°).

Each sensor was tested in six different configurations, as shown in Fig. 5, to test first the response of each channel and then of both at the same time.

An amplification circuit with a gain of 10 was connected to the outputs of the Wheatstone bridge. This circuit contains an instrumentation amplifier that helps with noise filtering and sets a reference voltage at 2.6 V. Any voltage below or above the reference voltage meant an imbalance in the Wheatstone bridge, caused by a change in resistance for the strain gauges.

[1] https://www.block.eu/en_US/productversion/cul-100010/

[2] www.agnthos.se

[3] https://www.xyztec.com/en/condor-sigma/

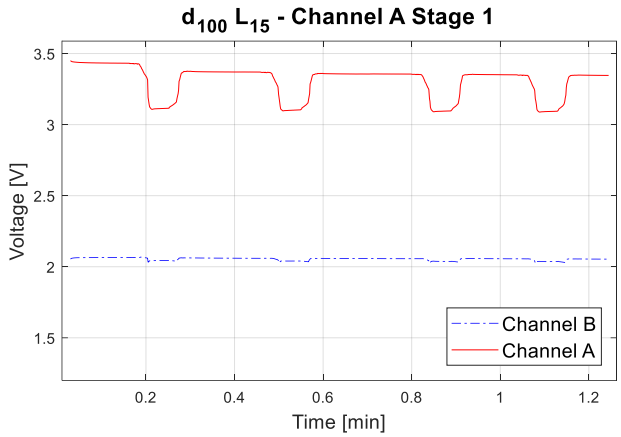

Fig. 6 Measurement results for channel A, stage one for the platin sensor with 100 µm thick extrusion channel and 15 µm long strain gauges.

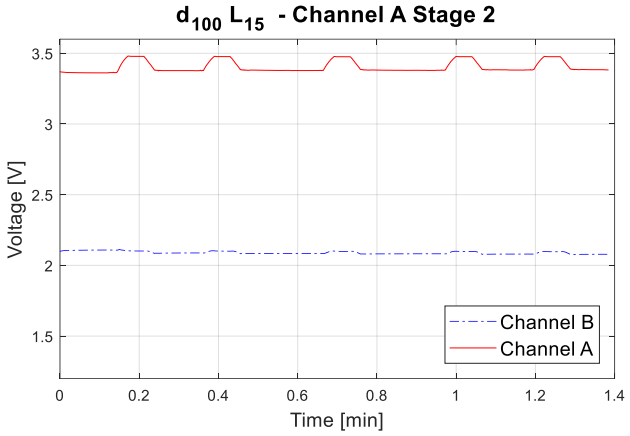

Fig. 9 Measurement results for channel A, stage two for the platin sensor with 100 µm thick extrusion channel and 15 µm long strain gauges.

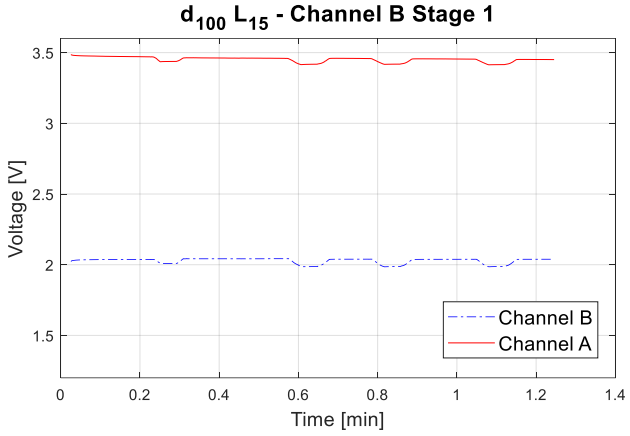

Fig. 7 Measurement results for channel B, stage one for the platin sensor with 100 µm thick extrusion channel and 15 µm long strain gauges.

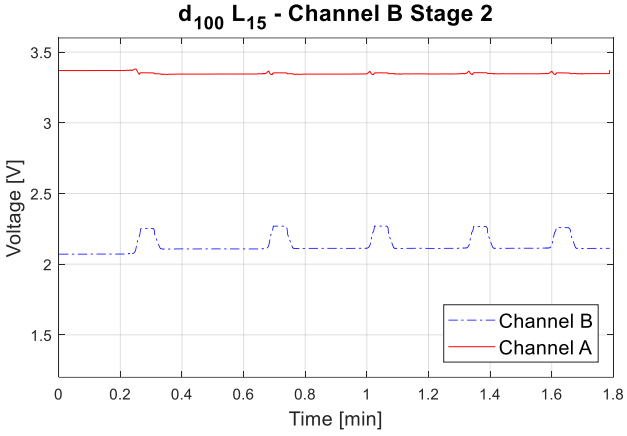

Fig. 10 Measurement results for channel B, stage two for the platin sensor with 100 µm thick extrusion channel and 15 µm long strain gauges.

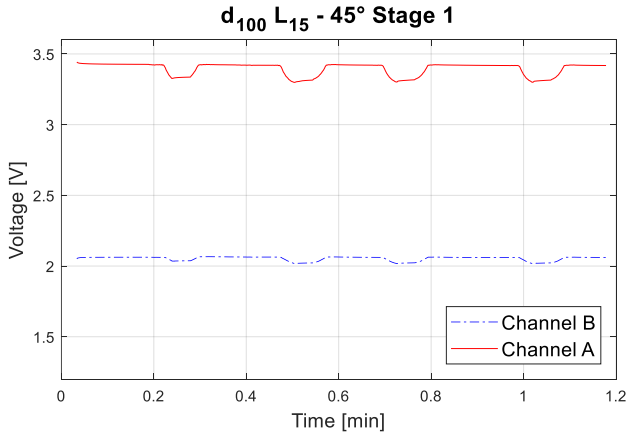

Fig. 8 Measurement results for the test at 45°, stage one for the platin sensor with 100 µm thick extrusion channel and 15 µm long strain gauges.

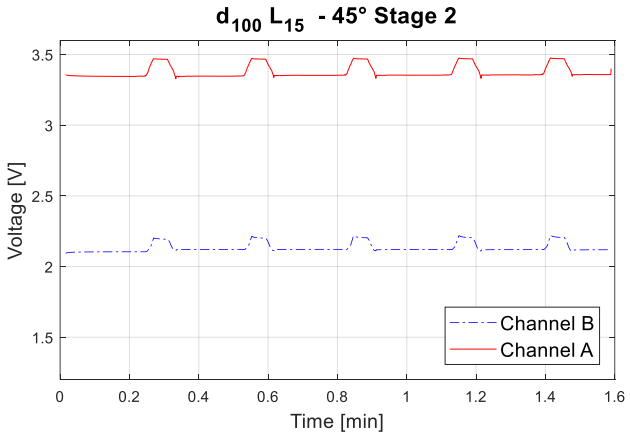

Fig. 11 Measurement results for the test at 45°, stage two for the platin sensor with 100 µm thick extrusion channel and 15 µm long strain gauges.

This change in voltage can be translated in a deformation of the hair.

The sensors with 10 µm long strain gauges were often damaged while measuring or while inserting the hair in the extrusion channel and showed comparably low sensitivity and less stability. Therefore, all designs with 10 µm long strain gauges will not be investigated.

Typical plots of one sensor are shown in Fig. 6 to Fig. 11. The measurements correspond to a sensor with a 100 µm thick extrusion channel and 15 µm long platin strain gauges (name convention $d_{100}L_{15}$). Similar results were seen for all sensors with strain gauges of 15 µm, 20 µm and 30 µm long.

The sensors with a 120 µm thick extrusion channel show a higher sensitivity than the 100 µm sensors, however, these suffer damage more often or give an unstable response during measurements. The reason behind this behavior is yet to be investigated.

In the measurement results shown in Fig. 6 to Fig. 11 it can be seen that one channel can have a different response amplitude to the same stimulus in different directions (see Fig. 6 and Fig. 9). Small cross-talk between both channels can also be appreciated in Fig. 7. These problems could be explained due to a misalignment during fabrication, the extrusion channel for the hair is not perfectly centered (see Fig. 12). Therefore, the strain gauges are asymmetrically deflected, showing a different response.

Fig. 12 Gold sensor with 120 µm extrusion channel and 30 µm long strain gauges. The extrusion channel is not properly centered, leading to measurement problems.

Another factor that could be affecting the measurement results is the gluing of the sensor on the PCB, where small angular misalignments can occur. This leads to the sensor

The sensitivity of each channel was calculated independently for each one of the six configurations (see Fig. 13), considering the deformation of the tip of the hair as input and the output voltage of the Wheatstone bridge as output.

The standard deviation for each configuration shown in Fig. 14 is approximately 0.2 V/m for channel A and 0.31 V/m for channel B. However, if we consider all measurements, the standard deviation increases drastically to 1.92 V/m for channel A and to 1.53 V/m for channel B, as shown in Fig. 14.

An average sensitivity of 5.46 V/m for channel A and 3.27 V/m for channel B can be seen in Fig. 14.

The variations in sensitivity seen in each measurement can be explained considering the measurement setup. For each configuration (sensor orientation in Fig. 5), the sensor is manually placed next to the metal hook that pulls the hair upwards (see Fig. 4).

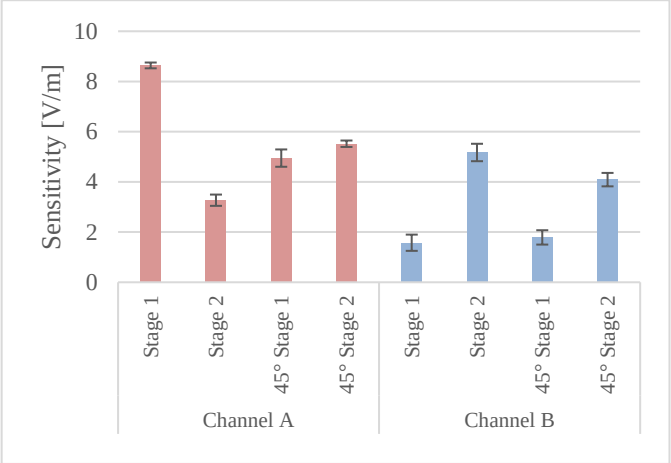

Fig. 13 Calculated sensitivity with standard deviation for the $d_{100}L_{15}$ platin sensor. Sensitivity was calculated for each configuration shown in Fig. 5.

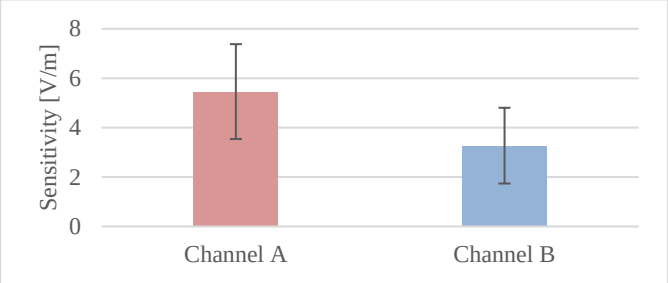

Fig. 14 Average sensitivity with standard deviation for the $d_{100}L_{15}$ platin sensor.

This leads to small variations in the hair position with respect to the hook, meaning that the deformation of the strain gauges is different for each measurement.

Other factor that might affect the repeatability of the measurements is the change in the elastic properties of the materials after an initial deformation.

5. Conclusions

This paper presents the sensing part of a self-healing flow sensor system that mimics the hair flow sensors found in nature. The system consists of four strain gauges embedded on a flexible substrate that lean on the base of an artificial hair and detect the surrounding flow.

Initial tests with the presented sensors show that it is possible to measure the direction and magnitude of a flow.

Further work must be done during the fabrication of the sensors to improve the alignment of the extrusion channel with respect to the strain gauges.

A method to reproducibly test the sensors must be defined, where the deflection of the strain gauges is equal for every test. Future tests inside a wind channel will be carried out to determine the working range of the sensor for detecting air currents.

The data presented in this paper shows promising results in the development of the first self-healing biomimetic hair flow sensor.

References

[1] Heys JJ, Rajaraman PK, Gedeon T and Miller J P. A Model of Filiform Hair Distribution on the Cricket. PLoS ONE 2012. v. 7 p. 1-12.

[2] Miller J, Krueger S, Heys JJ and Gedeon T. Quantitative Characterization of the Filiform Mechanosensory Hair Array on the Cricket Cercus. PLoS ONE 2011. v. 6.

[3] McConney ME, Chen N, Lu D, Coombs S, Liub C and Tsukruk VV. Biologically inspired design of hydrogel-capped hair sensors for enhanced underwater flow detection. Soft Matter 2009. v. 5. p. 292-295.

[4] Tao J and Yu B. Hair flow sensors: From bio-inspiration to bio-mimicking - A review. Smart Materials and Structures. 2012. v. 21.

[5] Liu YF, Huang P, Li YQ, Liu Q, Tao JK, Xiong DJ, N. Hu, C. Yan and H. W. a. S.-Y. Fu, "A biomimetic multifunctional electronic hair," *Journal of Materials Chemistry A*, vol. 7, no. 4, p. 1889-1896, 2019.

[6] Krijnen GJM, Dijkstra M, Baar JJ, Shankar SS, Kuipers WJ, Boer RJHd, Altpeter D, Lammerink TSJ and Wiegerink R. MEMS based hair flow-sensors as model systems for acoustic perception studies. Nanotechnology 2006. v. 17. p. 84-89.

[7] Dagamseh A, Bruinink C, Droogendijk H, Wiegerink R, Lammerink T and Krijnen aG. Engineering of Biomimetic Hair-Flow Sensor Arrays Dedicated to High-Resolution Flow Field Measurements. Hawai: IEEE Sensors 2010.

[8] Electronic Tutorials. Wheatstone Bridge. Aspencore, [Online]. Available: https://www.electronics-tutorials.ws/blog/wheatstone-bridge.html. [Accessed 19 02 2020].

[9] Hoffmann K. Applying the Wheatstone Bridge Circuit. Hottinger Baldwin Messtechnik GmbH 2009.

[10] Hair's breadth. Wikipedia, the free encyclopedia [Online]. Available: https://en.wikipedia.org/wiki/Hair%27s_breadth. [Accessed 11 02 2020].